Pergamon

PII: S0277-5387(98)00104-1

*Polyhedron* Vol. 17, No. 17, pp. 3005–3020, 1998

0277–5387/98 $19.00+0.00

# Manganese carboxylate clusters: from structural aesthetics to single-molecule magnets[1]

Guillem Aromí,[a] Sheila M. J. Aubin,[b] Milissa A. Bolcar,[a] George Christou,[a]* Hilary J. Eppley,[a] Kirsten Folting,[a] David N. Hendrickson,[b] John C. Huffman,[a] Rachel C. Squire,[a] Hui-Lien Tsai,[b] Sheyi Wang[a] and Michael W. Wemple[a]

[a]Department of Chemistry and Molecular Structure Center, Indiana University, Bloomington, IN 47405-4001, U.S.A

[b]Department of Chemistry, University of California at San Diego, La Jolla, CA 92093, U.S.A

(Received 13 February 1998)

**Abstract**—An overview is provided of some recent developments in manganese carboxylate cluster chemistry. A variety of synthetic methodologies are described together with the structures of the resultant products, which span metal nuclearities of 4 to 18 and oxidation states of II to IV, including mixed-valency. The spins of the ground states of these products are often large and sometimes abnormally large, and in certain cases when this is coupled to a sufficiently large magnetoanisotropy, the clusters function as single-molecule magnets i.e., they can be magnetized by an external magnetic field below a critical temperature. These complexes display hysteresis in magnetization *vs.* magnetic field studies, and clear evidence for quantum tunnelling of magnetization. Such results establish single-molecule magnetism as a new magnetic phenomenon, and one that holds great promise for next-century technological applications. © 1998 Elsevier Science Ltd. All rights reserved

## INTRODUCTION

Over the last decade or so, manganese carboxylate cluster chemistry has proved to be a rich source of a variety of polynuclear species. To date, metal nuclearities of up to 18 have been encountered in discrete form, and the Mn oxidation states have spanned the range II–IV, including mixed valency. The metal ions are invariably bridged by combinations of $O^{2-}$, $HO^-$ and $RO^-$ ions, and occasionally by one or both oxygen atoms of carboxylate groups. The stimuli for these studies have been varied and have included (i) the search for models of Mn-containing proteins and enzymes, in which Mn nuclearities up to 4 have been identified [1]; and (ii) the realization that Mn clusters often possess large (and occasionally abnormally large) values of ground state spin ($S$) [2], leading to a desire to understand the factors that yield this property and, in turn, stimulating the development of synthesis methodologies that might yield such species on a regular basis.

In a previous report during the early years of our efforts in Mn carboxylate chemistry [3], we described how the trinuclear, oxide-centered complexes $[Mn_3O(O_2CR)_6L_3]^z$ ($z = 0$, $Mn^{II}$, $2Mn^{III}$; $z = +1$, $3Mn^{III}$) were an excellent starting point for the synthesis of species with nuclearities up to 12. In the intervening years, a number of new synthesis procedures have been developed, several of which will be summarized herein. We shall also describe the magnetic properties of selected species and show how the high spin value exhibited by some of them leads to these complexes displaying the new magnetic phenomenon of single-molecule magnetism, which was indeed initially identified in Mn carboxylate chemistry. For

[1] Dedicated to Professor Jack Lewis on the occasion of his 70th birthday.

* Author to whom correspondence should be addressed.

consistency with the theme of this Symposium-in-Print, we shall only describe complexes with nuclearities $\geqslant 4$.

## SYNTHETIC METHODS

### *Aggregation of* $[Mn_4O_2]^{8+}$ *butterfly complexes*

One family of complexes that had been frequently encountered in earlier work was that containing a $[Mn_4O_2]^{8+}$ core with a planar or butterfly-like $Mn_4$ unit and $\mu_3-O^{2-}$ ions. Thus, the species $[Mn_4O_2(O_2CR)_7(L\text{-}L)_2]^z$ had been prepared and characterized, and contain peripheral ligation provided by bridging $RCO_2^-$ and chelating L-L (bipyridyl (bpy) [4], or the anions of picolinic acid ($pic^-$) [5], 8-hydroxyquinoline ($hqn^-$) [6], 2-hydroxymethylpyridine ($hmp^-$) [6] or dibenzoylmethane ($dbm^-$) [7]. These complexes were studied in detail by a variety of methods but did not represent good starting points to higher nuclearity species until the related complex $(NBu^n_4)[Mn_4O_2(O_2CPh)_9(H_2O)]$ (**1**; $4Mn^{III}$) was synthesized (Fig. 1) [7, 8]: the anion contains a $[Mn_4O_2]^{8+}$ butterfly unit with only $H_2O$ and $PhCO_2^-$ peripheral groups, and it has consequently proven a superb stepping stone to other species. A few examples of its use for this purpose will be described.

Addition of $Me_3SiCl$ destabilizes **1** by carboxylate abstraction and causes a nuclearity change to yield $(NBu^n_4)[Mn_8O_6Cl_6(O_2CPh)_7(H_2O)_2]$ (**2**; $8Mn^{III}$) [7, 9], whose anion is shown in Fig. 2. Such a transformation must clearly involve a complicated series of fragmentation/aggregation steps and equilibria, and the formation and isolation of **2** is undoubtedly facilitated by its low solubility that causes it to crystallize from solution. This is a common theme in many syntheses of higher nuclearity Mn species, and also rationalizes the often observed sensitivity of the product identity to the exact reaction conditions (i.e., carboxylate, solvent, etc.) which likely alter the relative solubilities of solution species in equilibrium. The structure of

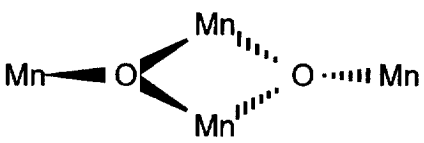


planar

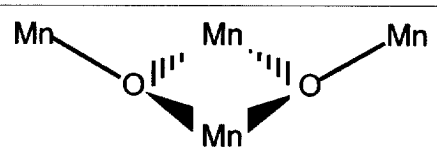


butterfly

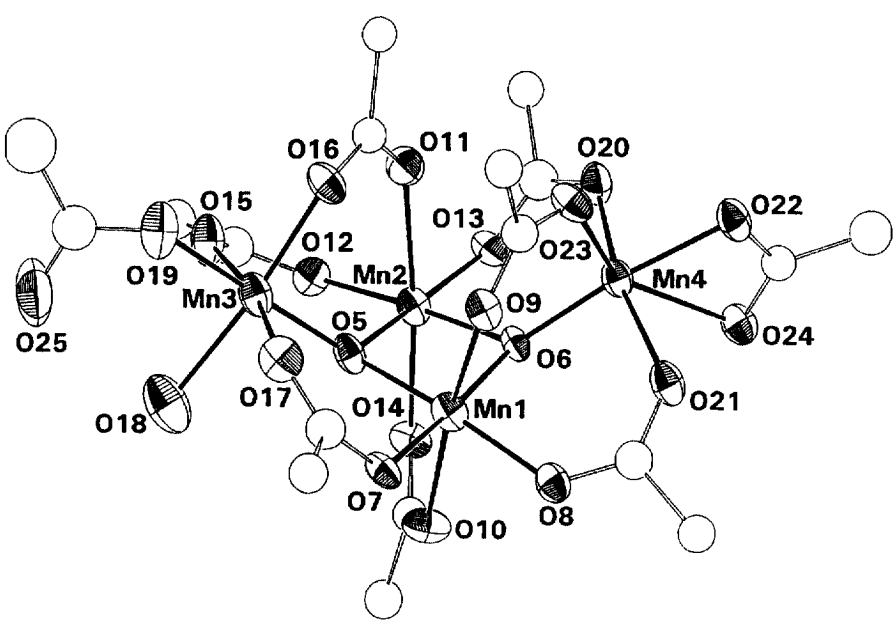


Fig. 1. The structure of the $[Mn_4O_2(O_2CPh)_9(H_2O)]^-$ anion of complex **1**.

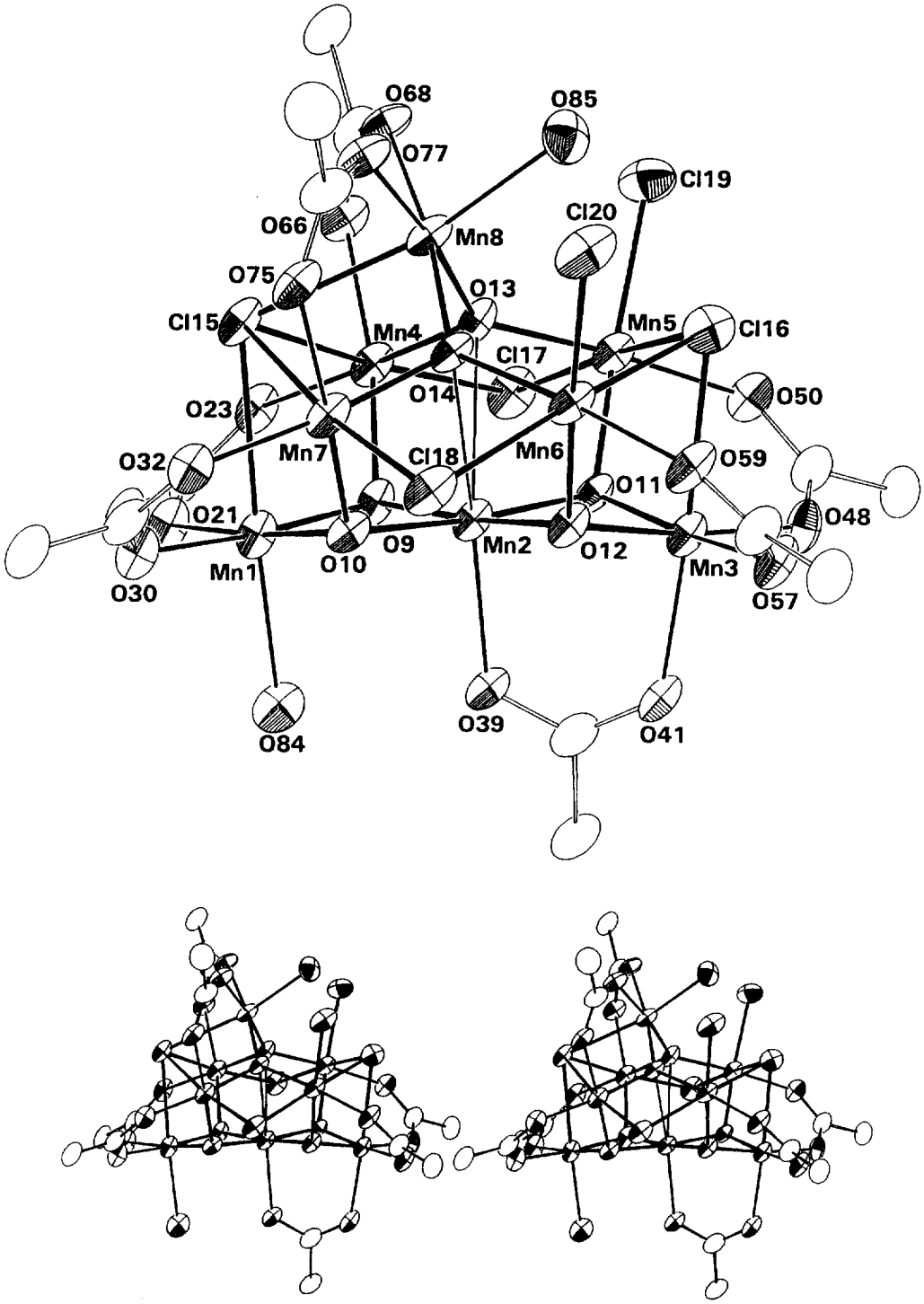


Fig. 2. The structure of the $[Mn_8O_6Cl_6(O_2CPh)_7(H_2O)_2]^-$ anion of complex **2**.

**2** consists of two body-fused butterfly units sharing central Mn(2), and an eighth metal atom, Mn(8), is held to the four wingtip Mn atoms by oxide bridges O(13) and O(14).

Another way of destabilizing complex **1** to aggregation is addition of benzoyl peroxide $(PhCO_2)_2$, which again gives a higher nuclearity product $[Mn_9Na_2O_7(O_2CPh)_{15}(MeCN)_2]$ (**3**; $9Mn^{III}$) [9] but no increase in the Mn oxidation level (of the isolated product, at least). The structure (Fig. 3) again comprises two body-fused butterfly units as in **2**, but now with two additional Mn atoms attached to the wingtip

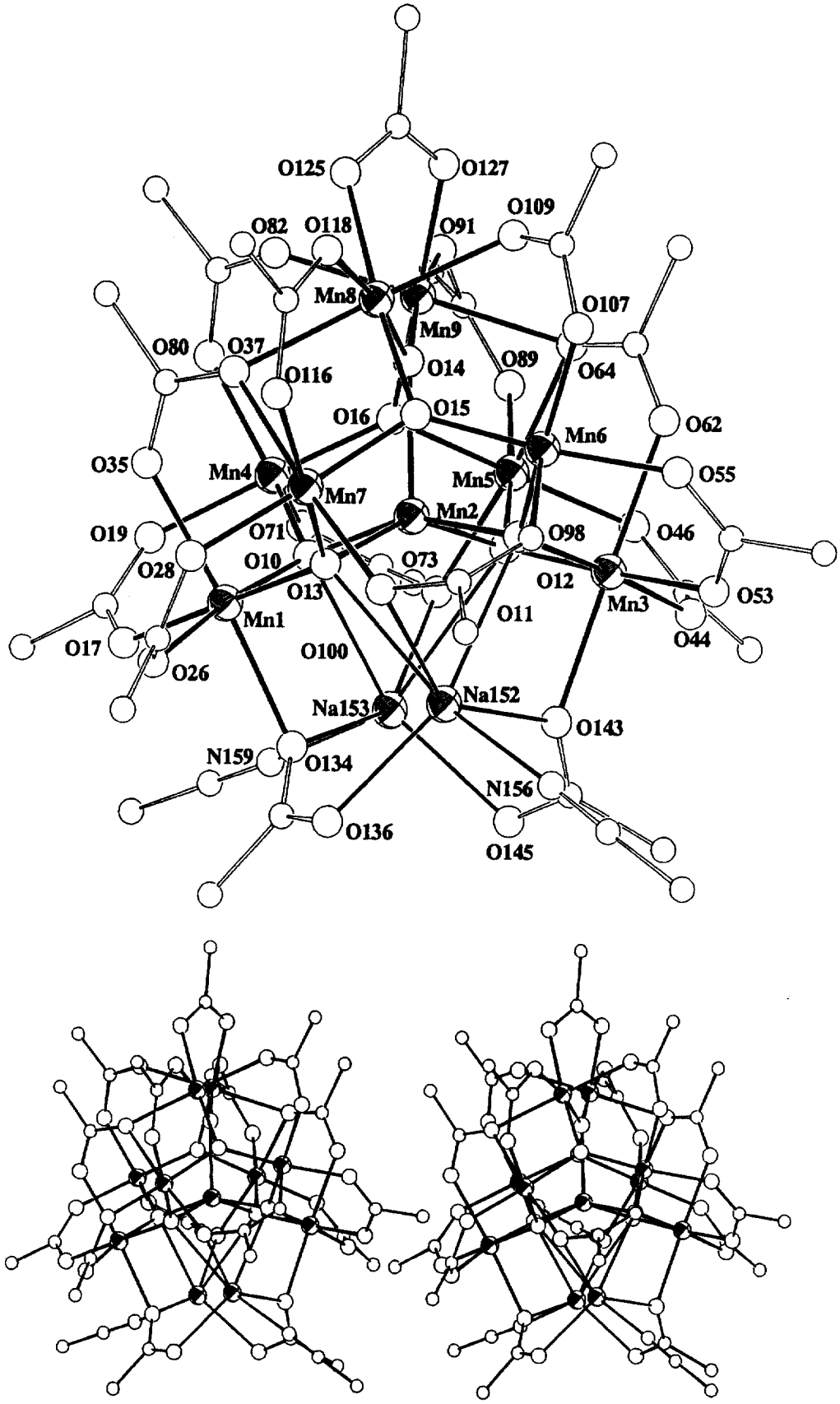


Fig. 3. The structure of $[Mn_9Na_2O_7(O_2CPh)_{15}(MeCN)_2]$ (**3**).

positions by three $O^{2-}$ ions O(14)–O(16). The $Na^+$ ions are intimately attached to the $[Mn_9O_7]$ unit and the system is best described as a mixed-metal cluster. A related complex with the same core structure but without $Na^+$ ions, $[Mn_9O_7(O_2CPh)_{13}(py)_2]$, has been made by Armstrong and coworkers [10].

The reactions of complex **1** with appropriate dicarboxylates was envisaged as a potential way of bringing two or more $[Mn_4O_2]$ units into close proximity and thereby possibly triggering aggregation into a higher nuclear product. Two particularly interesting successes of this strategy can be described. The reaction of **1** with 2,2-diethylmalonate ($Et_2mal^{2-}$) gives $(NBu^n_4)_2[Mn_8O_4(O_2CPh)_{12}(Et_2mal)_2(H_2O)_2]$ (**4**; $2Mn^{II}$, $6Mn^{III}$) [8] whose structure (Fig. 4) clearly demonstrates that its $[Mn_8O_4]$ core can be described as two linked $[Mn_4O_2]$ butterfly units. The $Et_2mal^{2-}$ groups provide additional inter-butterfly linkages and thus no doubt contribute to the formation and stabilization of an octanuclear species, presumably by initially forming a species in which two separate $[Mn_4O_2]$ complexes are bridged by a $Et_2mal^{2-}$ group. In contrast, the reaction of complex **1** with KH(phth) (phth = phthalate) causes a transformation to the octadecanuclear cluster $[K_4Mn_{18}O_{16}(O_2CPh)_{22}(phth)_2(H_2O)_4]$ (**5**; $18Mn^{III}$) [11] shown in Fig. 5. This remarkable structure can nevertheless be considered as the result of the linkage of several $[Mn_4O_2]$ units, and the two $phth^{2-}$ groups are $\mu_4$ and bridge a total of six $Mn^{III}$ ions between them, no doubt a contributing factor to the high nuclearity of the product.

A final example of a high nuclearity product from a $[Mn_4O_2]$ complex is provided by the dissolution of $[Mn_4O_2(O_2CPh)_6(MeCN)_2(pic)_2]$ in $Me_2NCOMe$ (DMA); black crystals of $[Mn_{10}O_8(O_2CPh)_6(pic)_8]$ (**6**; $10Mn^{III}$) slowly form (Fig. 6) [12]. This interesting transformation only occurs in DMA and is presumably caused by the good donor solvent destabilizing the $[Mn_4O_2]$ species to aggregation by partial or complete displacement of one or more carboxylate groups; again the low solubility of the product undoubtedly assists attainment of pure material.

*Controlled potential electrolysis*

The previous observation in our group that $[Mn_4O_2(O_2CMe)_6(py)_2(dbm)_2]$ ($4Mn^{III}$) would disproportionate to $[Mn_4O_3X(O_2CMe)_3(dbm)_3]$ ($X = Cl^-$ or $Br^-$; $3Mn^{III}$,$Mn^{IV}$) on treatment with

$$3[Mn_4O_2]^{8+} + 2X^- \rightarrow 2[Mn_4O_3X]^{6+} + 2Mn^{2+} + 2Mn^{3+} \quad (1)$$

$Me_3SiX$ in $CH_2X_2$ (eq. (1)) [8, 13] prompted an investigation of the electrochemical oxidation of selected $[Mn_4O_2]^{8+}$ species as a potentially useful method of forming similar or related products. Controlled potential electrolysis (CPE) of $[Mn_4O_2(O_2CMe)_6(py)_2(dbm)_2]$ at 0.84 V *vs.* ferrocene in the presence of dbmH gave $[Mn_4O_3(O_2CMe)_4(dbm)_3]$ (**7**; $3Mn^{III}$, $Mn^{IV}$) [14]. Similarly, the CPE of $(NBu^n_4)[Mn_4O_2(O_2CPh)_7(dbm)_2]$ at 0.65 V gave $[Mn_4O_3(O_2CPh)_4(dbm)_3]$ (**8**; $3Mn^{III}$, $Mn^{IV}$) [15]. In both cases, the one-electron oxidation of the $[Mn_4O_2]^{8+}$ core has triggered incorporation of a third $O^{2-}$ group, presumably from $H_2O$, and a change to a $[Mn_4(\mu_3\text{-}O)_3(\mu_3\text{-}O_2CR)]^{6+}$ core. This is summarized for **8** in eq. (2); a related equation summarizes the formation of **7**. The structures of **7**

$$[Mn_4O_2(O_2CPh)_7(dbm)_2]^- + dbmH - e^- + H_2O \rightarrow [Mn_4O_3(O_2CPh)_4(dbm)_3] + 3PhCO_2H \quad (2)$$

and **8** (Figs 7 and 8) are similar to those of $[Mn_4O_3X(O_2CMe)_3(dbm)_3]$ in possessing a trigonal pyramidal core with $O^{2-}$ ions on three faces and the basal face of $3Mn^{III}$ ions capped by a $\mu_3$-$X^-$ or $RCO_2^-$ ion. The R = Me (**7**) and Ph (**8**) species differ slightly, however, in that the former has a $\eta^1,\mu_3 - MeCO_2^-$ and the latter a $\eta^2,\mu_3 - PhCO_2^-$, the difference being assigned to the larger size of Ph *vs.* Me causing steric problems with the dbm Ph groups in a $\eta^1$, $\mu_3$-bridging mode for the R = Ph case.

Access to complex **7** in particular has allowed site-selective ligand substitution reactions at the $\mu_3 - MeCO_2^-$ position to be developed, a process facilitated by the $\mu_3 - MeCO_2^-$ group lying at the intersection of the three $Mn^{III}$ Jahn–Teller elongation axes and thus being more weakly bound and more susceptible to electrophilic attack by trimethylsilyl or related reagents than the other ligands in the molecule. Crystallographically confirmed products are shown in Fig. 9 [13–17], and others are currently being characterized.

*Comproportionation reactions*

A useful way of obtaining $Mn_x$ products at the ~III oxidation level is the comproportionation between a $Mn^{II}$ source and $MnO_4^-$. This was the original method used by Lis to access the dodecanuclear complex $[Mn_{12}O_{12}(O_2CMe)_{16}(H_2O)_4]\cdot 2H_2O\cdot 4MeCO_2H$ (**9**; $8Mn^{III}$, $4Mn^{IV}$) [18], the complex which has since initiated the field of Single-Molecule Magnetism (*vide infra*). Thus, the reaction of $Mn(O_2CMe)_2\cdot 4H_2O$ and $KMnO_4$ in 60% (v/v) $MeCO_2H/H_2O$ gives **9** *via* the comproportionation summarized in eq. (3). From **9** can now be made a variety of derivatives by

$$44Mn^{2+} + 16Mn^{7+} \rightarrow 5[Mn_{12}]^{40+} \quad (3)$$

ligand substitution reactions with other carboxylic acids eq. (4) [19, 20]; the R = Ph complex [19] is shown in Fig. 10. All these $Mn_{12}$ complexes are trapped-valence and contain a central

$$[Mn_{12}O_{12}(O_2CMe)_{16}(H_2O)_4] + 16RCO_2H \rightarrow [Mn_{12}O_{12}(O_2CR)_{16}(H_2O)_4] + 16MeCO_2H \quad (4)$$

$[Mn^{IV}_4O_4]$ cubane around which is a non-planar ring

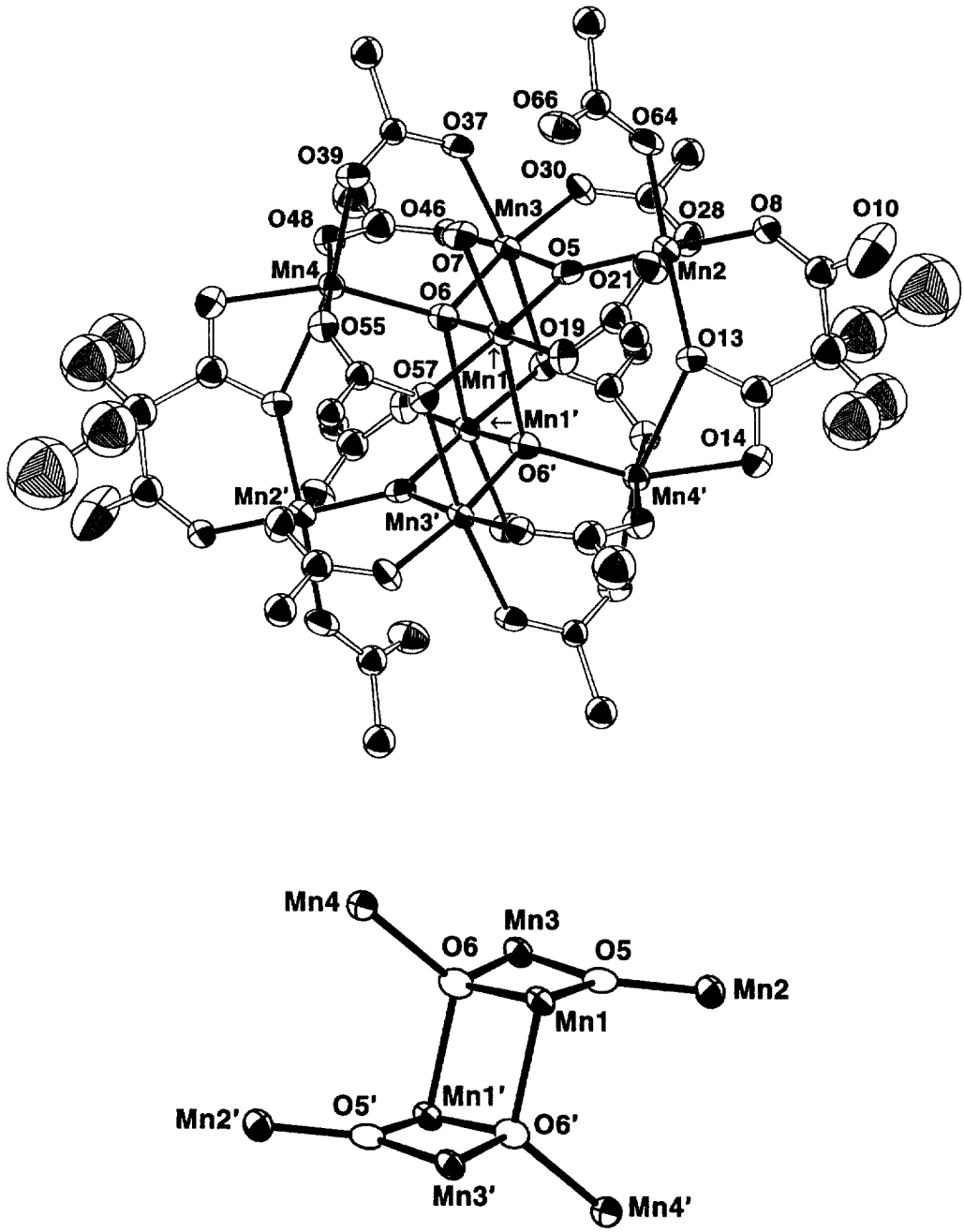


Fig. 4. The structure of $[Mn_8O_4(O_2CPh)_{12}(Et_2mal)_2(H_2O)_2]^{2-}$ anion and its $[Mn_8O_4]^{14+}$ core; the $Mn^{II}$ ions are Mn4 and Mn4'.

of $Mn^{III}$ ions held to the central cubane by eight $O^{2-}$ ions.

The $[Mn_{12}O_{12}(O_2CR)_{16}(H_2O)_4]$ complexes display a reversible one-electron reduction in the 0.00 to 0.50 V *vs.* ferrocene range, and this has allowed [20] isolation and characterization of the one-electron reduced clusters from reductions with $I^-$. Thus, for example, $(PPh_4)[Mn_{12}O_{12}(O_2CEt)_{16}(H_2O)_4]$ (**10**) can be prepared *via* eq. (5), a method that can readily be extended to other carboxylates [20].

$$[Mn_{12}] + PPh_4I \rightarrow (PPh_4)[Mn_{12}] + 1/2I_2 \qquad (5)$$

The comproportionation method has recently been employed to access a new $Mn_7$ complex. Treatment of $MnCl_2 \cdot 4H_2O$ with 2-hydroxymethylpyridine (hmpH) and $NEt_4MnO_4$ leads to $(NEt_4)[Mn_7(OH)_3Cl_3(hmp)_9]$

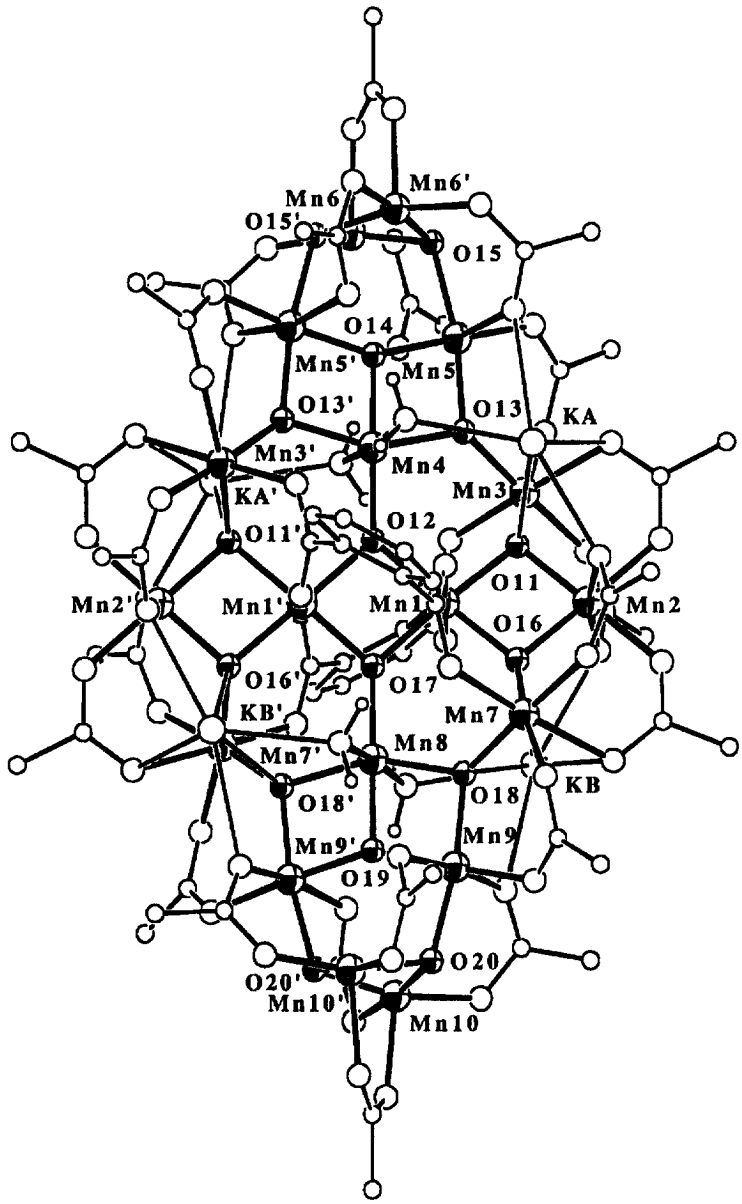


Fig. 5. The structure of $[K_4Mn_{18}O_{16}(O_2CPh)_{22}(phth)_2(H_2O)_4]$ **5**; the $K^+$ ions are labeled as KA and KB.

$(Cl)(MnCl_4)$ (**11**) [21], the $Mn_7$ anion of which (Fig. 11) contains $4Mn^{II}$, $3Mn^{III}$, the $Mn^{III}$ ions being easily identified from structural parameters and Jahn–Teller distortions as Mn(2), Mn(4) and Mn(6). Use of $MnBr_2{\cdot}4H_2O$ leads to the corresponding Br derivative, which is isostructural. Interestingly, the reaction of hmpH with the $Mn^{III}$ species $[Mn_3O(O_2CMe)_6(py)_3](ClO_4)$ leads to $[Mn_{10}O_4(OH)_2(O_2CMe)_8(hmp)_8](ClO_4)_4$ (**12**) [22], the cation of which (Fig. 12) is related to, but nevertheless distinctly different from that of **11**. Both **11** and **12** contain almost planar $Mn_x$ cores held together by bridging $O^{2-}/OH^-$ ions, with peripheral ligation provided by bridging $hmp^-$ and (for **12**) $MeCO_2^-$ groups.

## MAGNETIC PROPERTIES

*Ground state spin value*

It has become evident over the course of the last several years that small values of spin, $S$, in the ground states of Mn carboxylate clusters are almost the exception rather than the rule [2]. For example, in Table 1 are listed the $S$ values for the $Mn_x$ carboxylate species mentioned in this paper, and although clusters with $S = 0$ are present, noteworthy is the significant number of large $S$ values in this list: for calibration, the largest $S$ for a molecular species is currently the $S = 33/2$ for one of the clusters in cocrystallized $Fe_{17}$

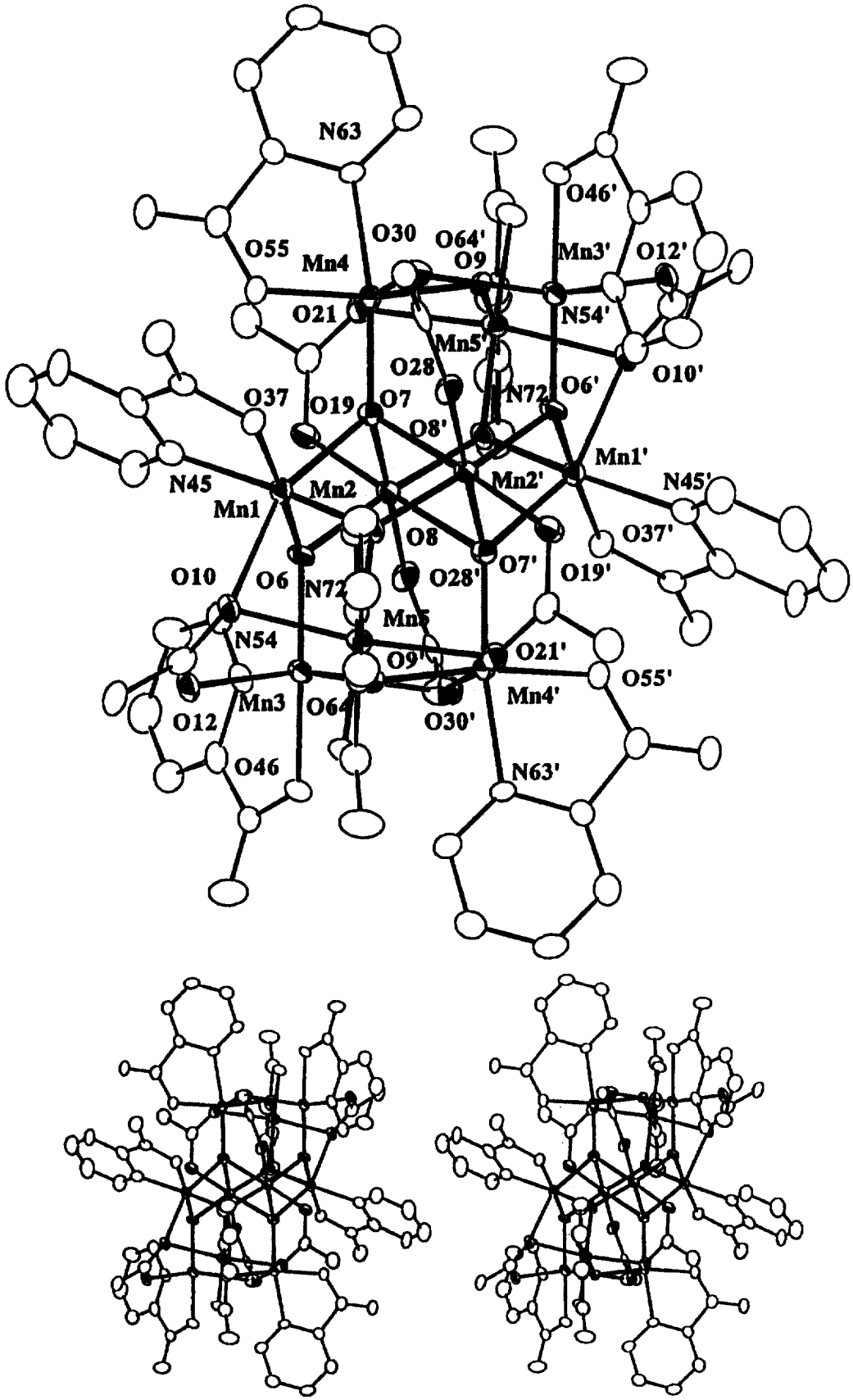


Fig. 6. The structure of $[Mn_{10}O_8(O_2CPh)_6(pic)_8]$ (**6**).

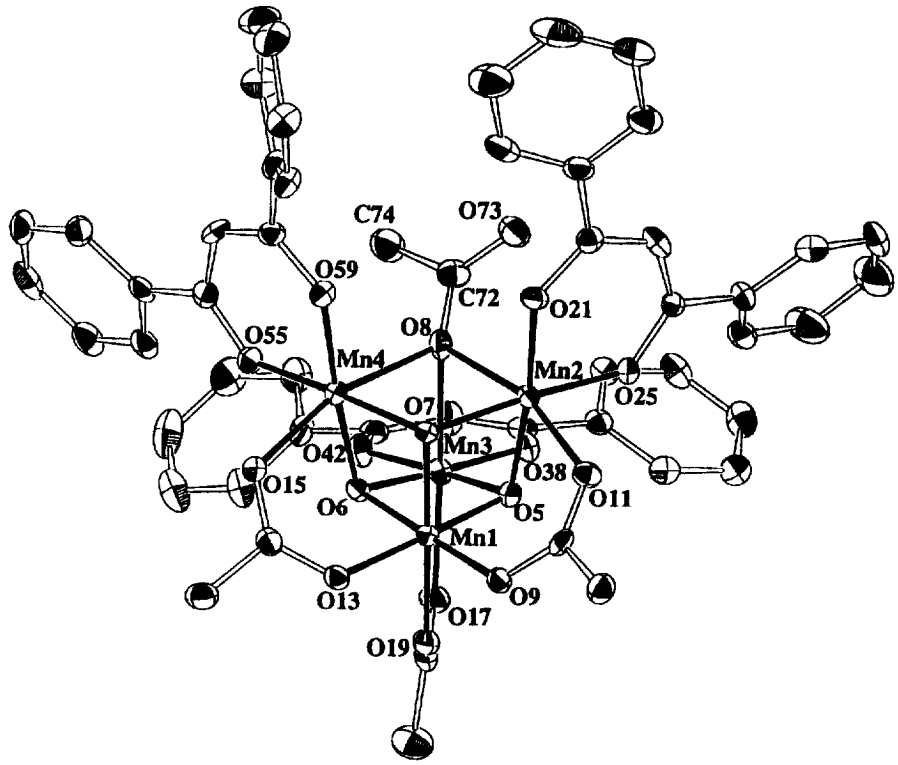


Fig. 7. The structure of $[Mn_4O_3(O_2CMe)_4(dbm)_3]$ (7).

and $Fe_{19}$ units [23]. The origin of the large $S$ value is a result of the presence of (at least some) ferromagnetic exchange interactions and/or spin frustration [24, 25] effects arising from the presence in certain topologies of competing exchange interactions. The latter prevent (frustrate) the preferred spin alignments that would otherwise normally yield low spin species.

For smaller clusters such as some of those in Table 1, the individual pairwise exchange parameters can be

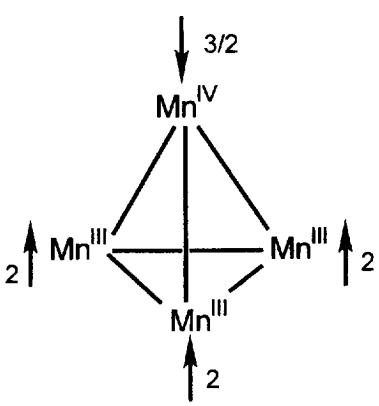


determined by fitting experimental molar magnetic susceptibility ($\chi_m$) *vs.* $T$ data to the appropriate theoretical equation derived for that topology and metal oxidation state(s) using the Kambe vector coupling methods [26]. In those cases, the ground state $S$ value may be readily rationalized. In other clusters, their complexity (size, symmetry) precludes such an analysis and only the value of the ground state may be obtained (*via* magnetization *vs.* field studies). An example of the former is found in the $[Mn_4O_3X]^{6+}$ species, which contain a $3Mn^{III},Mn^{IV}$ pyramid of $C_{3v}$ symmetry [13]. The $Mn^{III}/Mn^{III}$ exchange interactions ($J_{33}$) are ferromagnetic ($+5$ to $+10\,cm^{-1}$) and the $Mn^{III}/Mn^{IV}$ interactions ($J_{34}$) are antiferromagnetic ($-20$ to $-30\,cm^{-1}$), and the alignment of the individual $Mn^{III}$ and $Mn^{IV}$ spins (2 and 3/2, respectively) in the ground state are as shown, giving the molecular spin as $S = 6-3/2 = 9/2$, as is found experimentally.

An example of the latter approach is provided by the $[Mn_{12}O_{12}(O_2CR)_{16}(H_2O)_4]$ clusters, which have $S = 10$ ground states, except for a few, such as the R = Et species, which have $S = 9$ [19, 20]. The ground state may be rationalized as resulting from ferromagnetic exchange interactions within the central $[Mn_4O_4]$ cubane and antiferromagnetic interactions between central $Mn^{IV}$ and outer $Mn^{III}$ ions (although none of the $J$ values are actually known). This predicts a ground state of $S = 16-6 = 10$ since all the $Mn^{IV}$ and $Mn^{III}$ spins would be parallel and antiparallel, respectively. For complexes **2**–**6**, even this level of rationalization is not possible given the complex $Mn_x$ topology. Many competing exchange interactions of comparable magnitude and resultant spin frustration effects are undoubtedly present, and the observed

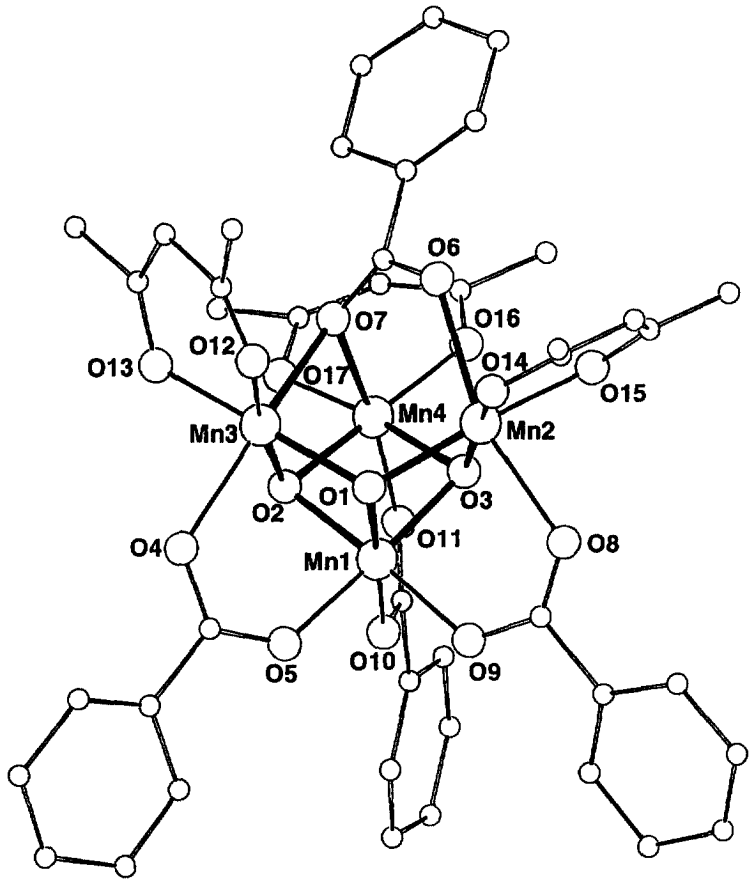


Fig. 8. The structure of $[Mn_4O_3(O_2CPh)_4(dbm)_3]$ (**8**).

ground states must therefore be a delicate balance of several factors. The latter makes it extremely difficult, in general, to predict in advance what the ground state might be of a new structural type, although some rationalization of the measured value is usually possible with hindsight, and this can still be a very useful level of understanding to possess.

A case in point is provided by complex **11** [21], whose ground state $S = 10$ or 11 may be rationalized as due to competition between the various pairwise exchange interactions which all involve $Mn^{II}/Mn^{II}$ ($J_{22}$) or $Mn^{II}/Mn^{III}$ ($J_{23}$) pairs and are thus all expected

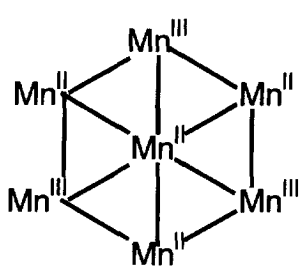


to probably be antiferromagnetic and very weak (and therefore of comparable magnitude). In particular, competition between $J_{io}$ and $J_{oo}$ (o = outer, i = inner), the former comprising both $J_{22}$ and $J_{23}$ and the latter only $J_{23}$, clearly prevents all spins aligning in an antiparallel arrangement. The resultant spin frustration thus gives a high spin ground state whose precise value must therefore be due to the relative magnitudes of the $J$ values. The interesting prediction that follows from this argument is that removal of the central Mn should give a non-frustrated system with antiparallel spin alignments around the hexagonal ring and a $S = 15/2 - 6 = 3/2$ ground state. Such a $[Mn^{II}_3Mn^{III}_3]$ cyclic species is not yet available to test this prediction but we note that $[Fe_6Na(OMe)_{12}(dbm)_6]^+$ has a hexagonal ring of $Fe^{III}$ ions, a central $Na^+$, and a $S=0$ ground state, as expected for a non-frustrated, antiferromagnetically-coupled system [27].

### *Single-molecule magnetism*

In 1993, it was discovered that the $[Mn_{12}O_{12}(O_2CMe)_{16}(H_2O)_4]\cdot 2H_2O\cdot 4MeCO_2H$ (**9**) complex could function as a nanoscale magnet [19, 28]. This initiated the field of molecular nanomagnetism and such a molecule has since been termed a single-molecule mag-

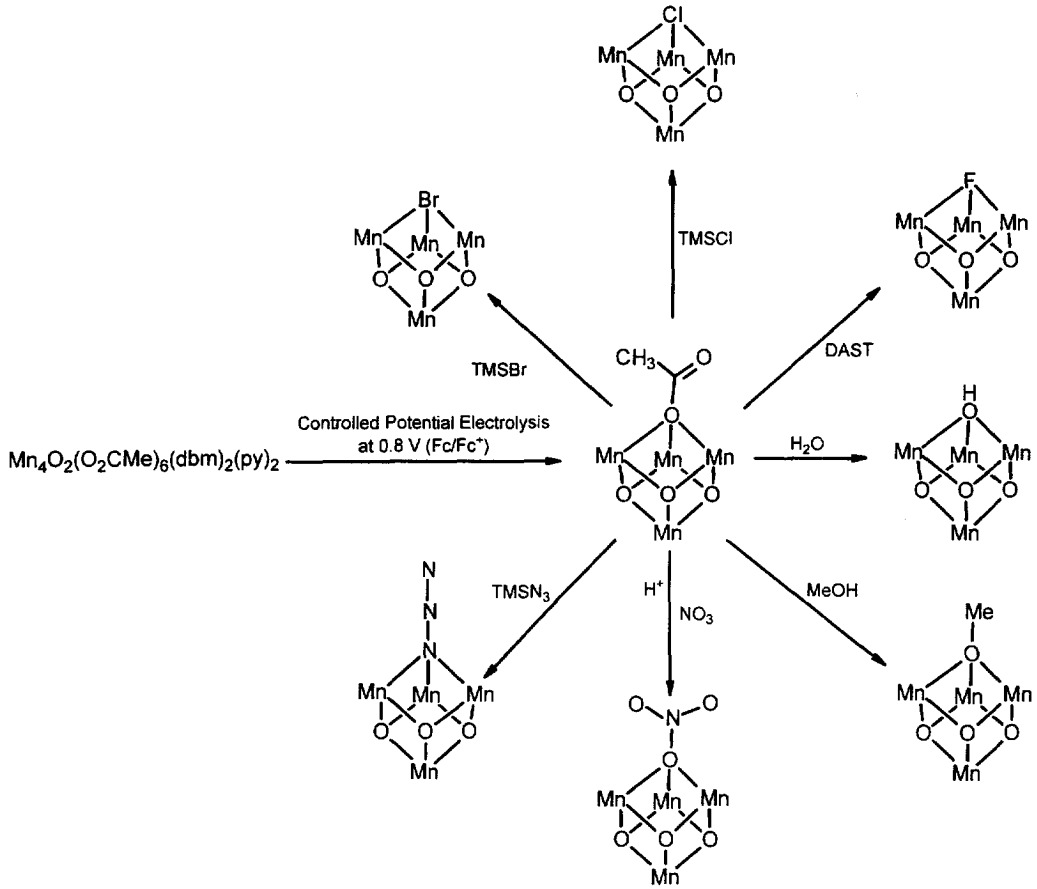


Fig. 9. Variation of X in structurally-characterized $[Mn_4O_3X]^{6+}$-containing products obtained from complex **7**. DAST is $Et_2NSF_3$; TMS is trimethylsilyl.

net (SMM) [29]. Nanoscale magnetic particles (nanomagnets) are typically of size 20–200 nm and are usually obtained by fragmenting bulk ferro- or ferrimagnets such as magnetite ($Fe_3O_4$), but this approach gives a distribution of particle sizes that complicates size *vs.* property studies and precludes a uniform response to an external influence such as an applied magnetic field. The discovery of SMMs in metal cluster chemistry represented an exciting breakthrough for a number of reasons: (i) metal clusters are normally prepared by solution methods and, once purified, such samples are composed of species of a

Table 1. state spin ($S$) values[1]

| Complex[a] | Ox. state | $S$ |
|---|---|---|
| $Mn_4O_3X(O_2CR)_3dbm)_3]$ (**7**,**8**) | $3Mn^{III}$, $Mn^{IV}$ | 9/2 |
| $[Mn_7(OH)_3Cl_3(hmp)_9]^{2+}$ (**11**) | $4Mn^{II}$, $3Mn^{III}$ | 10 or 11 |
| $[Mn_8O_6Cl_6(O_2CPh)_7(H_2O)_2]^-$ (**2**) | $8Mn^{III}$ | 11 |
| $[Mn_8O_4(O_2CPh)_{12}(Et_2mal)_2(H_2O)_2]^{2-}$ (**4**) | $2Mn^{II}$, $6Mn^{III}$ | 3 |
| $[Mn_9Na_2O_7(O_2CPh)_{15}(MeCN)_2]$ (**3**) | $9Mn^{III}$ | 4 |
| $[Mn_{10}O_8(O_2CPh)_6(pic)_8]$ (**6**) | $10Mn^{III}$ | 0 |
| $[Mn_{10}O_4(OH)_2(O_2CMe)_8(hmp)_8]^{4+}$ | $10Mn^{III}$ | 0 |
| $[Mn_{12}O_{12}(O_2CR)_{16}(H_2O)_4]$ (**9**) | $8Mn^{III}$, $4Mn^{IV}$ | 9 or 10 |
| $[Mn_{12}O_{12}(O_2CR)_{16}(H_2O)_4]^-$ (**10**) | $Mn^{II}$, $7Mn^{III}$, $4Mn^{IV}$ | 19/2 |
| $[K_4Mn_{18}O_{16}(O_2CPh)_{22}(phth)_2(H_2O)_4]$ (**5**) | $18Mn^{III}$ | 0 |

[a]For salts, only the $Mn_x$-containing ion is shown.

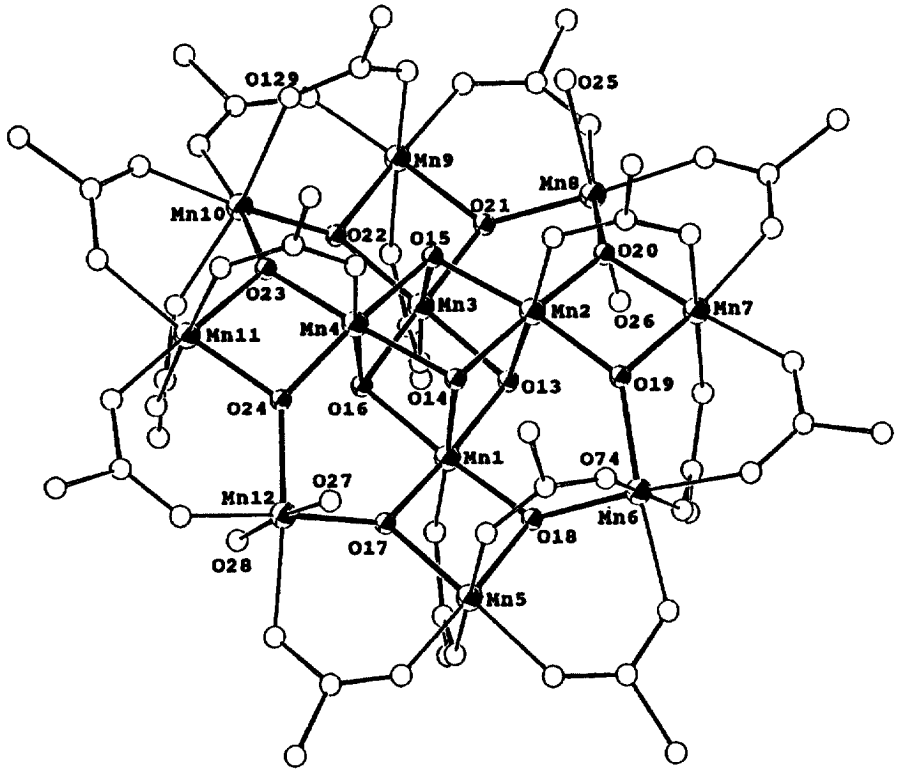


Fig. 10. The structure of $[Mn_{12}O_{12}(O_2CPh)_{16}(H_2O)_4]$; for clarity, only the *ipso* carbon atom of each Ph ring is shown.

single, sharply-defined size; (ii) they are readily amenable to variation in peripheral carboxylate ligation (small *vs.* bulky, hydrophilic *vs.* hydrophobic, etc.); (iii) they are normally soluble in common solvents providing advantages in potential applications, e.g., thin film formation (and removal); and (iv) they are, in fact, of sub-nanoscale dimensions—the $[Mn_{12}O_{12}]$ core of **9** has an approximate volume of only 0.1 $nm^3$. Points (i) and (iii) are major advantages of SMMs over conventional nanoscale magnetic particles, and point (iv) holds the promise of access to the ultimate high density memory device. Including the carboxylates, the volume of **9** is very approximately 2 $nm^3$, with a shape that can be described as a disc of circular surface area $\sim 2\,nm^2$ and thickness $\sim 1$ nm. Close packing could fit $\sim 5 \times 10^{13}$ clusters on a 1 $cm^2$ computer chip, at least four or five orders of magnitude greater than the highest density possible to date.

The SMM behavior of **9** and other carboxylate derivatives studied more recently is due to a combination of a large ground state spin $S$ and negative magnetoanisotropy as gauged by a negative zero-field splitting parameter $D$. As a result, there is a significantly large barrier for the reorientation of the cluster's magnetization vector. Thus, if an applied magnetic field is used to orient all the molecular magnetization vectors in one direction, the temperature lowered below a critical (or "blocking") temperature ($\sim 3$ K), and the field switched off, the magnetization vectors remain aligned and the sample is thus magnetized. The time scale of the magnetization relaxation is greater than two months.

More recently [20], the ionic species $(PPh_4)[Mn_{12}O_{12}(O_2CEt)_{16}(H_2O)_4]$ **10** and other carboxylate derivatives (such as the benzoate) have also been found to be SMMs, thus extending this new magnetic phenomenon to ionic species (i.e., "single-ion magnetism", although this alternate term has not been employed to date).

A characteristic signature of a magnet is hysteresis in the magnetization *vs.* magnetic field response, and representative examples are shown in Figs 13 and 14 for complex **10** [20, 30] and $[Mn_{12}O_{12}(O_2CC_6H_4\text{-}p\text{-}Me)_{16}(H_2O)_4]$ [31], respectively. Hysteresis of magnetization is clearly evident, confirming magnetic bistability and the appropriateness of the SMM description, but these figures also show two additional features that represent the focus of intense study at the present time. Considering Fig. 13 first, there are clear signs of steps on the hysteresis loop at regular intervals of magnetic field. Such steps were first seen for the $MeCO_2^-$ complex **9** [32] and are a signature of quantum tunnelling of the magnetization (QTM) i.e., instead of the cluster's magnetization relaxing from,

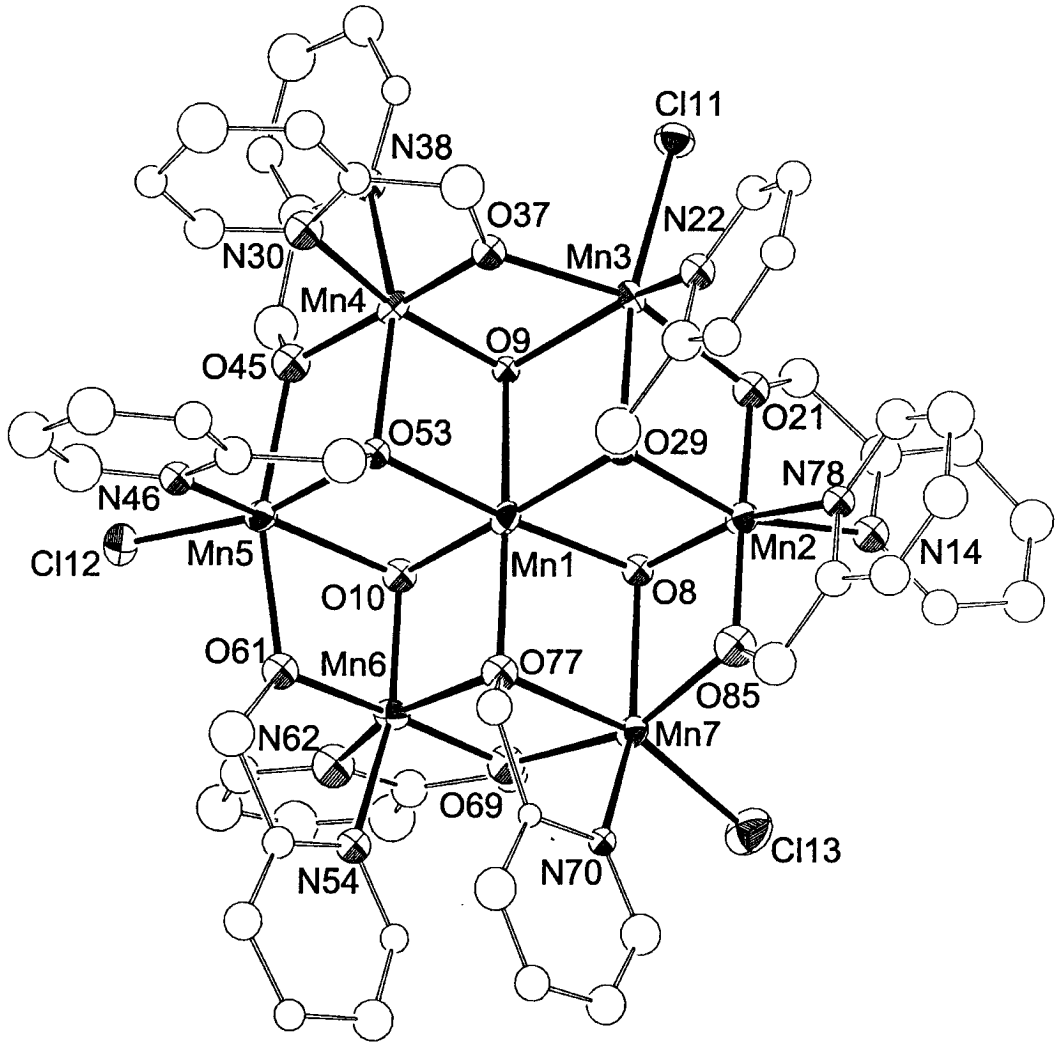


Fig. 11. The $[Mn_7(OH)_3Cl_3(hmp)_9]^{2+}$ cation of complex **11**.

say, "spin up" to "spin down" by going over the reorientation barrier, it instead tunnels through the barrier; more detailed discussion and analysis of the step behavior are available elsewhere [31–34]. In essence, these nanoscale clusters straddle the classical/quantum interface and thus allow study of how quantum mechanical behavior at the macroscopic scale underlies classical behavior at the macroscopic scale.

The hysteresis loops in Fig. 14 again show steps but also demonstrate a remarkable sensitivity of the hysteresis and QTM behavior to subtle differences resulting from two different crystal forms of the complex i.e., the $3H_2O$ solvate (space group $I2/a$) and the $HO_2CC_6H_4$-*p*-Me solvate (space group $C2/c$) [31]. The two crystal forms show significantly different step sizes, particularly the first step at zero field, which suggests that environmental differences in the two complexes have profound effects on the QTM rates. We have also found similar changes when the identity of the carboxylate is altered [34]. Such a significant sensitivity of the quantum behavior to readily-altered macroscopic parameters is important to understand and control, since this is likely to be important in future technological applications of SMMs.

One way to consider the $Mn_{12}$ SMMs is as extremely small pieces of a metal oxide stabilized and solubilized by the carboxylate ligands. It is often contemplated how small a piece of a 3D extended solid such as a metal oxide can become and still retain the essential properties of the bulk material. With respect to magnetic properties, it would appear that as few as 12 metal ions in the $[Mn_{12}O_{12}]$-containing complexes will suffice! It should be added that the $[Mn_{12}O_{12}]$ core is not an exact, repeating unit within a known Mn oxide. In fact, an even smaller molecule can also be a SMM.

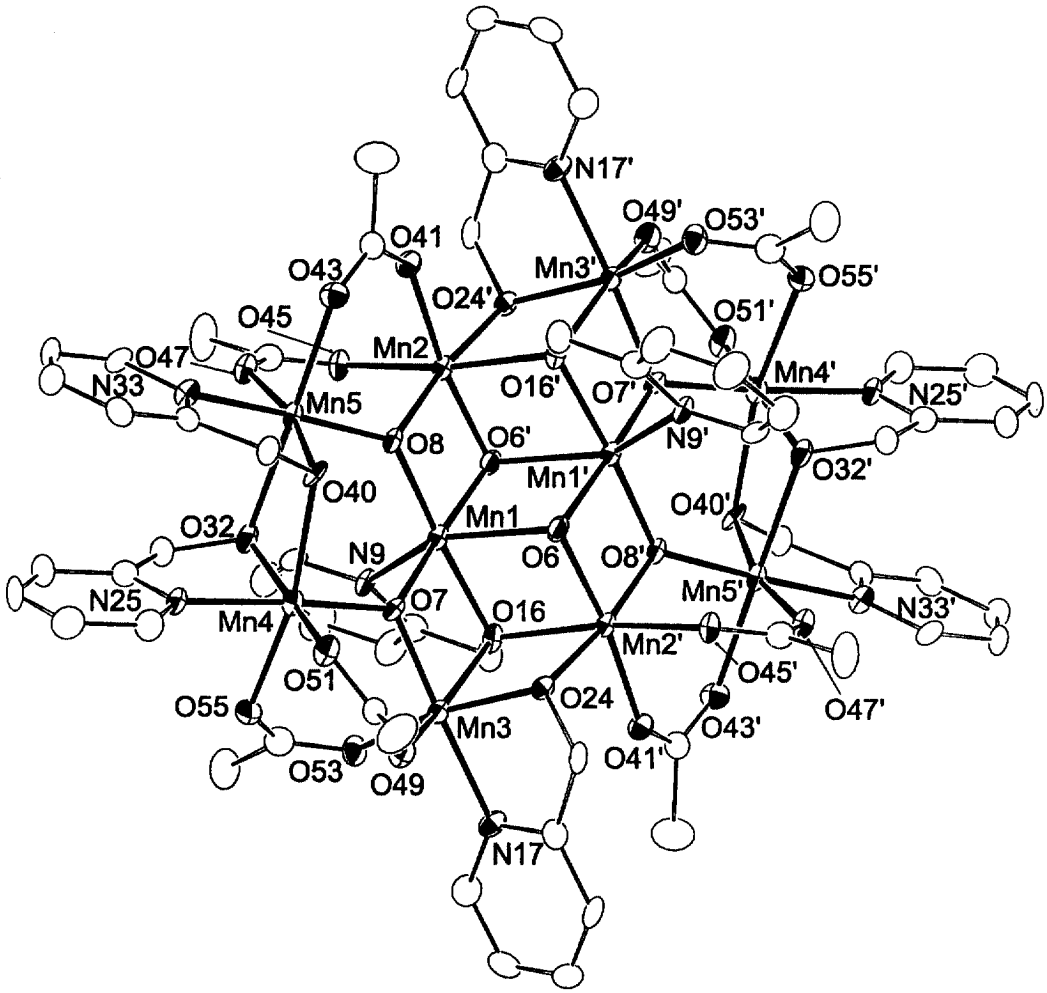


Fig. 12. The $[Mn_{10}O_4(OH)_2(O_2CMe)_8(hmp)_8]^{4+}$ cation of **12**.

The $[Mn_4O_3X]^{6+}$-containing clusters such as **7** have also been found to be SMMs, as reflected in the slow relaxation of magnetization [29], and the appearance [35] of a hysteresis loop *and* steps characteristic of QTM (Fig. 15). Lower temperatures are required, which is consistent with the smaller ground state spin of $S = 9/2$ for these clusters, as well as smaller $D$ values than for the $Mn_{12}$ species. Nevertheless, it firmly demonstrates that there is essentially no size minimum for the occurrence of SMM behavior; the $[Mn_4O_3X]$ core has a volume of $\sim 0.01\ nm^3$.

## CONCLUSIONS

Manganese carboxylate cluster chemistry has proven to be an area that has something for everyone, from synthetic chemistry and structural aesthetics to high-spin ground states and novel magnetic properties. The SMM behavior could not of course have been anticipated, and this area is thus a perfect example of a curiosity-driven line of "pure" research that leads to results of potentially major technological application. The temperatures required for SMM behavior in this first generation of examples are very low ($< 3$ K) but in this regard the field is at the same stage as superconductivity was when it was discovered in elemental mercury at liquid helium temperatures i.e., the important point is the establishment of the phenomenon and it will be up to future efforts in the field of SMMs to push the critical temperature to higher, more useful values. Other examples of SMMs both outside and within Mn chemistry are being reported [36, 37], but they are all like the $[Mn_4O_3X]$ species in requiring lower temperatures than the $[Mn_{12}O_{12}]$ complexes. However, the search has only just begun.

*Acknowledgements*—This research was supported by the U.S. National Science Foundation and National Institutes of Health.

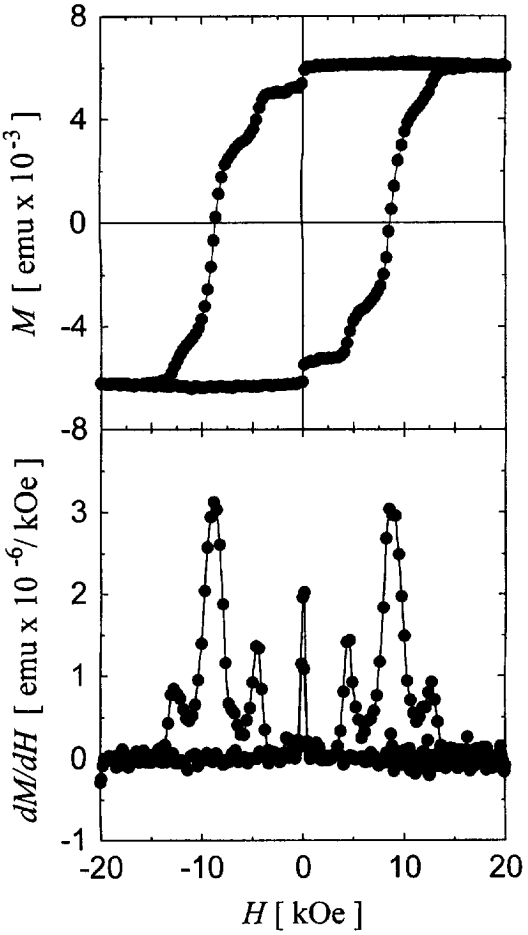


Fig. 13. (top) Magnetization hysteresis loop at 1.85 K for oriented crystals of $(PPh_4)[Mn_{12}O_{12}(O_2CEt)_{16}(H_2O)_4]$ (**10**); and (bottom) plot of the first derivative of the hysteresis loop emphasizing the positions of the steps.

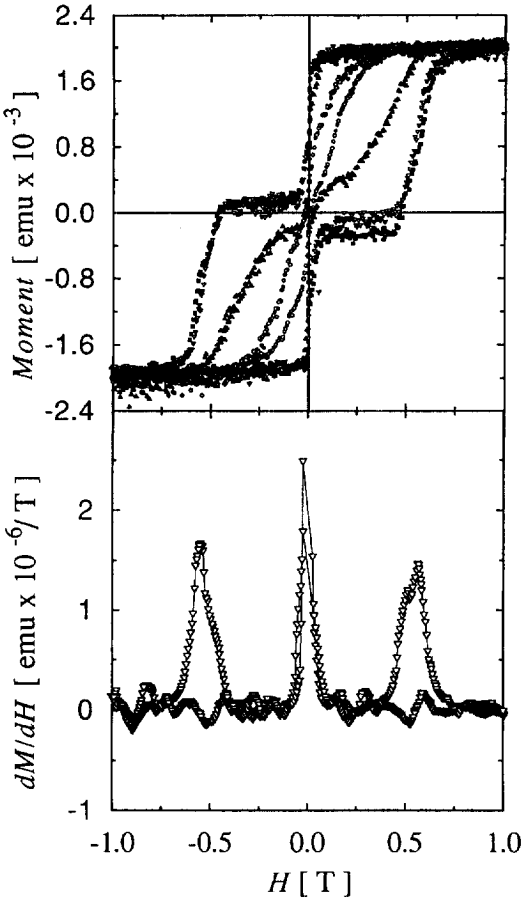


Fig. 15. (top) Magnetization hysteresis loop for oriented crystals of $[Mn_4O_3Cl(O_2CMe)_3(dbm)_3]$ at 0.426 (■), 0.53 (▽), 0.706 (△), and 0.90 K (○); and (bottom) the first derivative of the hysteresis loop.

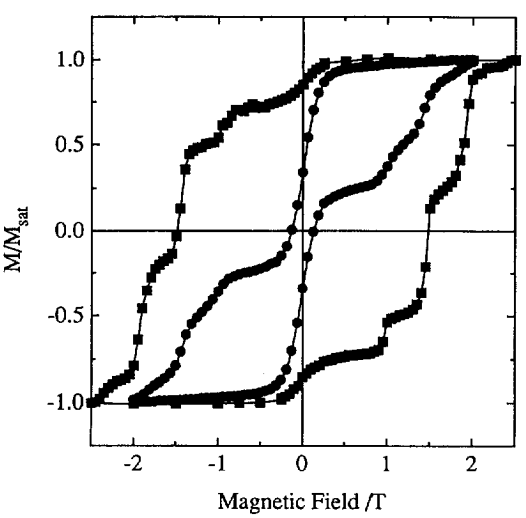


Fig. 14. Magnetization hysteresis loops at 1.90 K for oriented crystals of $[Mn_{12}O_{12}(O_2CC_6H_4\text{-}p\text{-}Me)_{16}(H_2O)_4]$ as the $3H_2O$ (■) or $HO_2CC_6H_4\text{-}p\text{-}Me$ (●) solvates.

## REFERENCES


1. (a) Yachandra. V. K., Sauer K. and Klein M. P., *Chem. Rev.* 1996, **96**, 2927. (b) Debus, J. R., *Biochim. Biophys. Acta* 1992, **1102**, 269.
2. Christou, G., in *Magnetism a Supramolecular Function*: ed. Kahn, O., NATO ASI Series; Kluwer, Dordrecht, The Netherlands, 1996, pp. 383–410.
3. Christou, G., *Acc. Chem. Res.*, 1989, **22,** 328.
4. Vincent, J. B., Christmas, C., Chang, H.-R., Li, Q., Boyd, P. D. W., Huffman, J. C., Hendrickson, D. N. and Christou, G., *J. Am. Chem. Soc.*, 1989, **111,** 2086.
5. Libby, E., McCusker, J. K., Schmitt, E. A., Folting, K., Hendrickson, D. N. and Christou, G., *Inorg. Chem.*, 1991, **30,** 3486.
6. Bouwman, E., Bolcar, M. A., Libby, E., Huffman, J. C., Folting, K. and Christou, G., *Inorg. Chem.*, 1992, **31,** 5185.
7. Wang, S., Huffman, J. C., Folting, K., Streib, W. E., Lobkovsky, E. B. and Christou, G., *Angew. Chem. Int. Ed. Engl.*, 1991, **30,** 1672.

8. (a) Wang, S., Folting, K., Streib, W. E., Schmitt, E. A., McCusker, J. K., Hendrickson, D. N. and Christou, G., *Angew. Chem. Int. Ed. Engl.*, 1991, **30**, 305. (b) Wemple, M. W., Tsai, H.-L., Wang, S., Claude, J.-P., Streib, W. E., Huffman, J. C., Hendrickson D. N. and Christou, G., *Inorg. Chem.*, 1996, **35**, 6437.
9. Tsai, H.-L., Wang, S., Folting, K., Streib, W. E., Hendrickson, D. N. and Christou, G., *J. Am. Chem. Soc.*, 1995, **117**, 2503.
10. Low, D. W., Eichhorn, D. M., Draganescu, A. and Armstrong, W. H., *Inorg. Chem.*, 1991, **30**, 878.
11. (a) Squire, R. C., Aubin, S. M. J., Folting, K., Streib, W. E., Hendrickson, D. N. and Christou, G., *Angew. Chem. Int. Ed. Engl.*, 1995, **34**, 887. (b) Squire, R. C., S. M. J. Aubin, Folting, K., Streib, W. E., Christou, G. and Hendrickson, D. N., *Inorg. Chem.*, 1995, **34**, 6463.
12. Eppley, H. J., Aubin, S. J. M., Streib, W. E., Bollinger, J. C., Hendrickson, D. N. and Christou, G., *Inorg. Chem.*, 1997, **36**, 109.
13. a) Wang, S., Tsai, H.-L., Streib, W. E., Christou, G. and Hendrickson, D. N., *J. Chem. Soc., Chem. Commun.*, 1992, 1427. (b) Wang, S., Tsai, H.-L., Folting, K., Streib, W. E., Hendrickson, D. N. and Christou, G., *Inorg. Chem.*, 1996, **35**, 7578.
14. Wemple, M. W., Adams, D. M., Folting, K., Hendrickson, D. N. and Christou, G., *J. Am. Chem. Soc.*, 1995, **117**, 7275.
15. Wang, S., Tsai, H.-L., Hagen, K. S., Hendrickson, D. N. and Christou, G., *J. Am. Chem. Soc.*, 1994, **116**, 8376.
16. Aromí, G., Folting, K., Huffman J. C. and Christou, G., (results to be published).
17. Aromí, G., Wemple, M. W., Aubin, S. M. J., Folting, K., Hendrickson, D. N. and Christou, G., *J. Am. Chem. Soc.*, (submitted for publication).
18. Lis, T., *Acta Cryst.*, 1980, **B36**, 2042.
19. Sessoli, R., Tsai, H.-L., Schake, A. R., Wang, S., Vincent, J. B., Folting, K., Gatteschi, D., Christou, G. and Hendrickson, D. N., *J. Am. Chem. Soc.*, 1993, **115**, 1804.
20. Eppley, H. J., Tsai, H.-L., de Vries, N., Folting, K., Christou, G. and Hendrickson, D. N., *J. Am. Chem. Soc.*, 1995, **117**, 301.
21. Bolcar, M. A., Aubin, S. M. J., Folting, K., Hendrickson, D. N. and Christou, G., *Chem. Commun.*, 1997, 1485.
22. Bolcar, M. A., Folting K. and Christou, G., (results to be published).
23. Powell, A. K., Heath, S. L., Gatteschi, D., Pardi, L., Sessoli, R., Spina, G., Del Giallo, F. and Pieralli, F., *J. Am. Chem. Soc.*, 1995, **117**, 2491.
24. To accommodate the comments of Kahn[25], expressions such as "spin frustration degeneracy" will be employed to describe the special case where competing exchange interactions lead to a degenerate ground state. In accord with our practice to date, we shall use "spin frustration" to describe the more general case where competing exchange interactions of comparable magnitude lead to the preferred spin alignments being prevented (frustrated).
25. Kahn, O., *Chem. Phys. Lett.*, 1997, **265**, 109.
26. Kambe, K., *J. Phys. Soc. Jpn.*, 1950, **5**, 48.
27. Caneschi, A., Cornia, A. and Lippard, S. J., *Angew. Chem. Int. Ed. Engl.*, 1995, **34**, 467.
28. Sessoli, R., Gatteschi, D., Caneschi, A. and Novak, M. A., *Nature*, 1993, **365**, 141.
29. Aubin, S. M. J., Wemple, M. W., Adams, D. M., Tsai, H.-L., Christou, G. and Hendrickson, D. N., *J. Am. Chem. Soc.*, 1996, **118**, 7746.
30. Aubin, S. M. J., Spagna, S., Eppley, H. J., Sager. R. E., Christou, G. and Hendrickson, D. N., *Chem. Commun.*, 1998, 803.
31. *Aubin, S. M. J., Sun, Z., Guzei, I. A., Rheingold, A. L., Christou, G. and Hendrickson, D. N., Chem. Commun.*, 1997, 2239.
32. Friedman, J. R., Sarachik, M. P., Hernandez, J. M., Zhang, X. X., Tejada, J., Molins, E. and Ziolo, R., *J. Appl. Phys.*, 1997, **81**, 3978.
33. (a) Tejada, J., Ziolo R. F. and Zhang, X. X., *Chem. Mater.*, 1996, **8**, 1784. (b) Thomas, L., Lionti, F., Ballou, R., Gatteschi, D., Sessoli R. and Barbara, B., *Nature*, 1996, **383**, 145.
34. Ruiz, D., Sun, Z., Albela, B., Folting, K., Ribas, J., Christou, G. and Hendrickson, D. N., *Angew. Chem. Int. Ed. Engl.*, 1998, **37**, 300.
35. Aubin, S. M. J., Dilley, N. R., Wemple, M. W., Maple, M. B., Hendrickson, D. N. and Christou, G., *J. Am. Chem. Soc.*, 1998, **120**, 839.
36. (a) Sun, Z., Grant, C. M., Castro, S. L., Hendrickson, D. N. and Christou, G., *Chem. Commun.*, 1998, 721. (b) Castro, S. L., Sun, Z., Grant, C. M., Bollinger, J. C., Hendrickson D. N. and Christou, G., *J. Am. Chem. Soc.*, 1998, **120**, 2977.
37. Barra, A. L., Debrunner, P., Gatteschi, D., Schultz, C. E. and Sessoli, R., *Europhys. Lett.*, 1996, **35**, 133.